ISSN 1063-7842, Technical Physics, 2013, Vol. 58, No. 7, pp. 1016–1024. © Pleiades Publishing, Ltd., 2013.
Original Russian Text © I.A. Lyashenko, 2013, published in Zhurnal Tekhnicheskoi Fiziki, 2013, Vol. 83, No. 7, pp. 87–95.

PHYSICAL SCIENCE OF MATERIALS

Effect of the Temperature Dependence of the Viscosity of Pseudoplastic Lubricants on the Boundary Friction Regime

I. A. Lyashenko

Sumy State University, ul. Rimskogo-Korsakova 2, Sumy, 40007 Ukraine
e-mail: nabla04@ukr.net

Received July 12, 2012

Abstract—The boundary friction regime appearing between two atomically smooth solid surfaces with an ultrathin lubricating layer between them is considered. The interrupted (stick-slip) regime of motion typical of the boundary lubrication is represented as a first-order phase transition between the structural states of the lubricant. The thermodynamic and shear melting is described. The universal dependence of the viscosity of high-molecular alkanes (lubricants) on the temperature and velocity gradient is taken into account. The dependence of the friction force on the lubricant temperature and the relative shear velocity of the interacting surfaces are analyzed. It is shown that the temperature dependence of the viscosity makes it possible to describe some experimentally observed effects. The possibility of prolonged damped oscillations after lubricant melting prior to the stabilization of the steady-state sliding mode is predicted. In the stick-slip regime in a wide range of parameters, a reversive motion is observed when the upper block moves in both directions after melting.

DOI: 10.1134/S106378421307013X

INTRODUCTION

Friction plays a special role in our everyday life because it is encountered continually. Owing to static friction, we can walk, hold things in our hands, the objects surrounding us remain in their places, and so on. In tribology, several basic regimes of friction are distinguished: dry friction (without lubrication); fluid friction between interacting surface divided by a layer of a lubricant of various thicknesses and origins; mixed (or semifluid) friction in the presence of regions of dry and fluid friction; and boundary friction in which the thickness of the lubricating layer is on the order of a few atomic diameters. As a rule, mixed friction regimes are realized in actual situations, which complicates their description. One of the main characteristics of friction is the friction coefficient depending on the nature of contacting surfaces and the lubricant. Lubrication regimes are often represented in the form of Hersey–Stribeck diagrams [1] illustrating the dependence of the friction coefficient on characteristics such as viscosity, velocity, and external load. On the classical diagram, the hydrodynamic, mixed, and boundary regimes change one another consecutively upon a decrease in the thickness of the lubricant. In 1902, Stribeck proposed a diagram named after him. With the development of experimental methods, it was found in the last decade that the boundary regime of friction is very complicated and has a number of peculiarities [2–4] that do not fit to the standard Hersey–Stribeck curve. In this connection, a new friction map generalizing the Hersey–Stribeck diagram was proposed on the basis of a large body of experimental data; the domain of boundary lubrication is represented in this chart in greater detail.

At present, a large number of experimental investigations are being carried out for studying boundary friction under various conditions. One of the important trends in these studies is analysis of the features of boundary friction processes in the presence of a molecularly-thin lubricant film between two atomically smooth solid surfaces [3–8]. One of the factors determining the topicality of investigation of such objects is rapid development of technologies for constructing nanosize mechanical systems that cannot be described by classical mechanics and require the development of new theories. Another reason is that in spite of the fact that idealized cases with atomically smooth surfaces and ultrathin homogeneous lubricating films are far from the conditions observed in traditional friction assemblies, experiments of this kind (both actual and computer experiments) make it possible to analyze the peculiarities of the boundary friction mode in the case when the effect of inhomogeneities in the lubricant and roughnesses of the surfaces can be minimized.

To describe the results of experiments on analysis of the boundary friction regime and nanocontact effects, the methods of molecular dynamics [9–11] as well as phenomenological models [12–15] are being actively used. In particular, in the synergetic model proposed in [16], the melting of the lubricating layer is governed by the mechanisms of thermodynamic and shear melting. Using this model, the effect of additive fluctuations of the main parameters of the lubricant in the

boundary mode was investigated and it was shown that their action leads to the formation of new stationary states and kinetic regimes of friction [17, 18]. Popov [12, 13] developed a thermodynamic theory of boundary friction based on the Landau theory of second-order phase transitions [19] in which the shear modulus of the lubricant assuming zero value in the liquid-like phase is chosen as the order parameter. However, publications [12, 13] have certain limitations because melting of the lubricant in them is described as a continuous second-order phase transition, while jumpwise first-order phase transformations [3, 5, 15] leading to stabilization of an interrupted mode of motion are often observed in the boundary friction regime [3–5]. In [20, 21], theory [12, 13] was generalized to the case of a first-order phase transition and the features of interrupted (stick–slip) regimes of boundary friction were analyzed on the basis of mechanical analogs of tribological systems of two types.

The models constructed in [20, 21] adequately describe the stick–slip friction mode and the factors leading to it; however, the dependence of the effective viscosity of the boundary lubricant only on the velocity gradient is taken into account, although the viscosity always depends on temperature. The absence of such a dependence makes it possible to analyze the behavior of the system upon a change in temperature only qualitatively because temperature still appears in the expansion of free energy [20, 21]. This study continues the investigations described in [20, 21] and aims at the generalization of the existing model and at analysis of the boundary friction regime taking into account the universal temperature dependence of the viscosity of solid alkanes [22]. It should be noted that the results of analysis of the effect of temperature on the boundary friction regime are rarely elucidated in the literature, and a comprehensive analysis carried out in [22] makes it possible to perform the generalization proposed in the present article.

1. FREE ENERGY

Let us write the expression for the free energy density for a homogeneous lubricant pressed between two atomically smooth surfaces in the form [12, 13, 20, 21]

$$f = \alpha(T - T_c)\varphi^2 + \frac{a}{2}\varphi^2\varepsilon_{el}^2 - \frac{b}{3}\varphi^3 + \frac{c}{4}\varphi^4, \qquad (1)$$

where T is the lubricant temperature, T_c is the critical temperature, ε_{el} is the elastic shear strain, and α, a, b, and c are positive constants. In expression (1), we introduced order parameter φ, which is the amplitude of the periodic part of the microscopic function of the density of the medium, to describe the phase state of the lubricant [12, 13]. In the liquid-like phase, there is no long-range order in alteration of atoms, and steady-state value of $\varphi_0 = 0$ sets in. If, however, the lubricant is solid-like, parameter φ assumes a nonzero value. Expansion (1) corresponds to the model of a first-order phase transition [19, 23].

Potential (1) have extrema defined as [20, 21]

$$\varphi_{\mp} = \frac{b}{2c} \mp \sqrt{\left(\frac{b}{2c}\right)^2 - \left(\frac{a}{c}\varepsilon_{el}^2 + \frac{2\alpha(T - T_c)}{c}\right)}, \qquad (2)$$

where φ_- corresponds to the maximum of potential (1) and φ_+ corresponds to its minimum. The values of φ_+ correspond to stationary states of the lubricant. In addition to condition (2), solution $\varphi_0 = 0$ corresponding to the extremum of the potential for zero value of the order parameter always exists (it can be a minimum, a maximum, or a plateau). In accordance with relation (2), melting of the lubricant (state with the stationary value $\varphi_0 = 0$) is equivalently attained in accordance with two mechanisms: conventional thermodynamic melting upon an increase in temperature T and the shear melting due to mechanical action upon an increase in the shear component of elastic strain ε_{el}.

Analysis of expression (2) makes it possible to determine the critical values of temperatures and strains for which a phase transition occurs in the system. For low values of temperature T and strain ε_{el}, the lubricant is solid-like because, in accordance with relation (2), a nonzero steady-state value of order parameter φ_0 is realized. In this case, the potential has the form shown by curve *1* in Fig. 1 (the stationary state corresponds to the minimum at $\varphi_0 > 0$).[1]

When temperature T exceeds the value

$$T_c^0 = T_c - \frac{a}{2\alpha}\varepsilon_{el}^2, \qquad (3)$$

the situation depicted by curve *2* in Fig. 1 is observed, where in addition to the minimum at $\varphi_0 > 0$, a potential minimum at $\varphi_0 = 0$ appears. However, since these minima are separated by a potential barrier (see the inset to the figure), no transition to state with $\varphi_0 = 0$ occurs, and the lubricant remains solid-like. Upon a further increase in temperature to values exceeding critical temperature

$$T_{c0} = T_c - \frac{a}{2\alpha}\varepsilon_{el}^2 + \frac{b^2}{8\alpha c}, \qquad (4)$$

the potential barrier disappears (curve *3* in Fig. 1), and the system abruptly passes to the state with $\varphi_0 = 0$ in accordance with the mechanism of the first-order phase transition; the lubricant melts thereby. If the temperature is decreased after melting, the lubricant abruptly solidifies at a temperature $T < T_c^0$ (3). Thus, melting of the lubricant occurs at a temperature $T > T_{c0}$ (4) and its solidification occurs at a lower value of

[1] Since the order parameter is the density modulation, its negative values have no physical meaning, and we will henceforth consider the region of $\varphi \geq 0$.

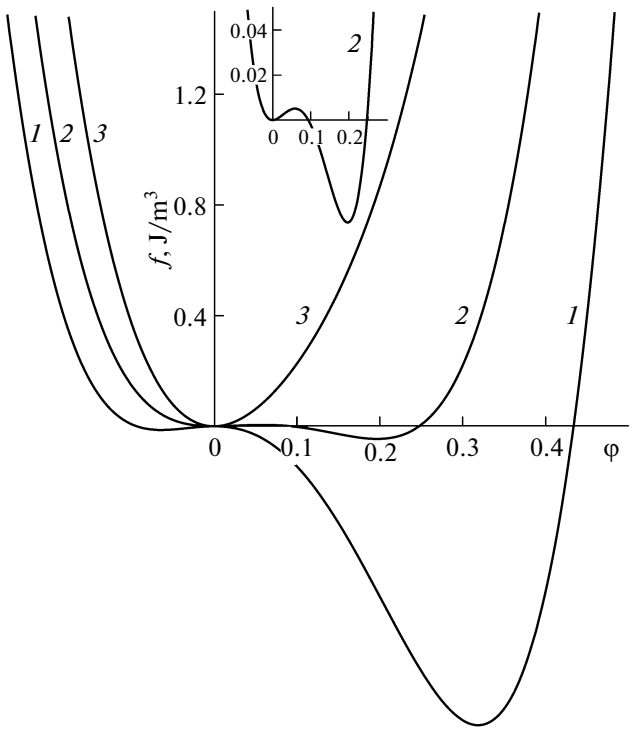

Fig. 1. Dependence of free energy density f (1) on order parameter φ (dimensionless quantity) for $\alpha = 0.95$ J K^{-1}/m^3, $T_c = 290$ K, $a = 2 \times 10^{12}$ Pa, $b = 230$ J/m^3, and $c = 900$ J/m^3. Curves *1–3* correspond to temperatures $T = 271$, 286, and 310 K, respectively, and strain $\varepsilon_{el} = 3 \times 10^{-6}$.

$T < T_c^0$ (3). Accordingly, the $\varphi_0(T)$ dependence exhibits a hysteresis loop in temperature [20, 21], its width

$$\Delta T = T_{c0} - T_c^0 = \frac{b^2}{8\alpha c} \quad (5)$$

being a function of only the expansion coefficients. Note that during melting, the order parameter changes jumpwise from its stationary value $\varphi_0 = 0.5bc^{-1}$ to zero, while during solidification it increases from zero to $\varphi_0 = bc^{-1}$.

In accordance with expressions (3) and (4), the lubricant also melts when the elastic strain ε_{el} appearing in it exceeds the critical value

$$\varepsilon_{el,c0} = \sqrt{\frac{2\alpha(T_c - T)}{a} + \frac{b^2}{4ac}} \quad (6)$$

and solidifies when the strain becomes smaller than

$$\varepsilon_{el,c}^0 = \sqrt{\frac{2\alpha(T_c - T)}{a}}. \quad (7)$$

2. ALLOWANCE FOR VISCOSITY AND FRICTION MAP

Let us define elastic stresses σ_{el} appearing in the lubricating layer as the derivative of free energy f with respect to strain ε_{el},

$$\sigma_{el} = \mu\varepsilon_{el}, \quad (8)$$

$$\mu = a\varphi^2, \quad (9)$$

where shear modulus μ of the lubricant can be reduced to the square of the order parameter to within a constant factor a [12, 13, 20, 21]. In addition to elastic stresses σ_{el}, viscous component σ_v also appears during motion of interacting surfaces. Friction force F opposing the motion is defined as the product of the total stresses by the area of the contact between the interacting surfaces:

$$F = (\sigma_{el} + \sigma_v)A. \quad (10)$$

Let us define the viscous stresses in the lubricant layer by the formula [4, 22]

$$\sigma_v = \eta_{eff}\dot{\varepsilon}, \quad (11)$$

where η_{eff} is the effective viscosity of the lubricant. In experiments on boundary friction, lubricating materials under investigation are usually polymer solutions and melts [3, 5]. This is due to the fact that the lubricant should not be squeezed from under the surfaces in the course of the experiment, which can be ensured more easily with long polymer molecules. Such lubricants are non-Newtonian pseudoplastic liquids. The viscosity of Newtonian liquids depends only on temperature, while the viscosity of non-Newtonian liquid is also a function of strain rate $\dot{\varepsilon}$ [4]. In contrast to dilatational liquids, viscosity η_{eff} for pseudoplastic liquids decreases with increasing $\dot{\varepsilon}$, which facilitates the reduction of friction.

The dependence of viscosity η_{eff} of linear alkanes containing from 20 to 1400 carbon atoms on the temperature and strain rate was investigated in [22] by the molecular dynamics method. Measurements were taken in the temperature range from 0 to 900 K. A lubricant layer of thickness $h \sim 3$ nm containing from 6 to 8 molecular monolayers pressed between smooth solids was analyzed (which corresponds to the object considered here). The authors of [22] succeeded in obtaining a universal dependence of the form

$$\log\eta_{eff} = C - n\log\dot{\varepsilon}, \quad (12)$$

where parameters C and n depend on the temperature. It can be seen from this expression that at low temperatures in the state of rest ($\dot{\varepsilon} = 0$), effective viscosity η_{eff} turns to infinity, which corresponds to a solid-like lubricant; however, this does not lead to a sharp increase in the friction force because, in accordance with relations (10) and (11), its viscous component vanishes in the state of rest ($\dot{\varepsilon} = 0$).

It was shown in [22] that a solid-like lubricant at low temperatures corresponds to $n = 1$, while upon an increase in temperature, the lubricant exhibits the standard Newtonian behavior with parameter $n = 0$. To describe this feature, the propose the dependence of the form

$$n = \frac{1}{1 + (T/T_k)^{\beta}}, \quad (13)$$

where constants T_k and β depend on the type of the polymer being used. In particular, these parameters for eicosane $C_{20}H_{42}$ are $T_k = 353$ K and $\beta = 4.09$ [22].

The $C(n)$ dependence for all types of polymer lubricants under investigation can be approximated by the equality [22]

$$C = 10.9n - 3.8. \quad (14)$$

Expressions (12)–(14) give the dependence of viscosity η_{eff} on temperature T and strain rate $\dot{\varepsilon}$. This dependence is shown as a 3D diagram (Fig. 2), where the temperature step of the mesh is 25 K and $\log\dot{\varepsilon}$ changes with a step of 0.5. The diagram shows that the viscosity decreases upon an increase in temperature and strain rate $\dot{\varepsilon}$. With increasing temperature, the dependence on $\dot{\varepsilon}$ becomes weaker because the value of parameter n tends to zero upon heating in accordance with relation (13), and viscosity (12) at $n = 0$ is Newtonian.

It was shown in [15, 20, 21, 24] that when the interacting surfaces separated by an ultrathin lubricant layer of thickness h move relative to each other with velocity V, steady-state elastic strains

$$\varepsilon_{el} = \frac{V\tau_\varepsilon}{h} \quad (15)$$

appear in the layer, where τ_ε is the Maxwellian relaxation time of internal stresses [12]. Expression (15) takes into account both elastic ε_{el} and plastic ε_{pl} strains emerging in the lubricant [15, 20, 21]. For a small value of τ_ε, for which the adiabatic approximation $\tau_\varepsilon\dot{\varepsilon}_{el} \approx 0$ holds, the running value of strain ε_{el} for a motion with a varying velocity V is also defined by expression (15) to a high degree of accuracy. To determine the strain rate, we will use the standard relation [4, 22]

$$\dot{\varepsilon} = \frac{V}{h}. \quad (16)$$

Combining the expressions given in Section 2, we obtain the computational formula for determining the total friction force

$$F = \left[a\varphi^2\tau_\varepsilon + 10^{10.9n-3.8}\left(\frac{V}{h}\right)^{-n}\right]\frac{AV}{h}, \quad (17)$$

where the steady-state value of φ is determined in accordance with Eq. (2) in which elastic strain ε_{el} is defined by expression (15). The latter expression makes it possible to generalize the results obtained in [15, 20, 21] because it takes into account the temperature dependence of viscosity. Note that expression (17) is in conformity with the results obtained by Epifanov [1, 25], who demonstrated that the increase in friction upon an increase in the load occurs due to an increase in the shear contact area A. However, expression (17) used here is independent of loading. This is due to the fact that we consider specific conditions of friction between two atomically smooth interacting surfaces separated by an ultrathin layer of the lubricant. In this case, the contact area is close to the area of the interacting surfaces irrespective of the applied pressure. The more so that in the case considered here, the distance h between the surfaces is maintained constant irrespective of the area of the surfaces. The modern experimental technique makes it possible to create such specific conditions. However, the interacting surfaces and the lubricant in actual mechanisms always have roughnesses; for this reason, the true contact area A will still increase with the load. This allows us to estimate the effect of pressure (load) on the behavior of the system by varying the value of A. Note that the pressure dependence was taken into account explicitly in [15, 26].

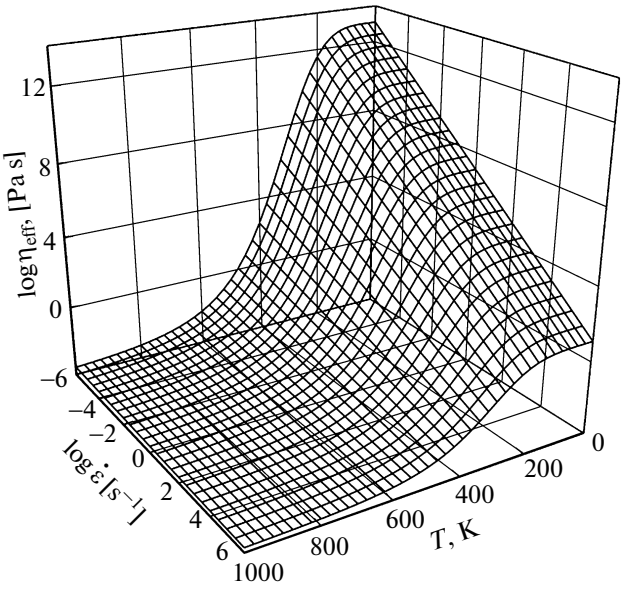

Fig. 2. Dependence of the logarithm of effective viscosity η_{eff} (12) of eicosane $C_{20}H_{42}$ on the logarithm of strain rate $\dot{\varepsilon}$ and temperature T for parameters $T_k = 353$ K and $\beta = 4.09$ [22].

Figure 3a shows the decrease in force of friction (17) upon an increase in temperature T, which occurs due to a decrease in the shear modulus μ defining the elastic component of force F as well as due to a decrease in viscosity η_{eff} that determines the viscous force of friction. After melting of the lubricant at temperature $T > T_{c0}$, the elastic component of force F becomes zero; however, the friction force continues to decrease due to a further decrease in the viscosity. An analogous figure was given in [21], where $F(T) = \text{const}$ after melting because the viscous component of F in [21] depends only on shear velocity V, and all curves in Fig. 3a are plotted for a fixed shear velocity. The $F(T)$ dependence obtained here demonstrates a sharper

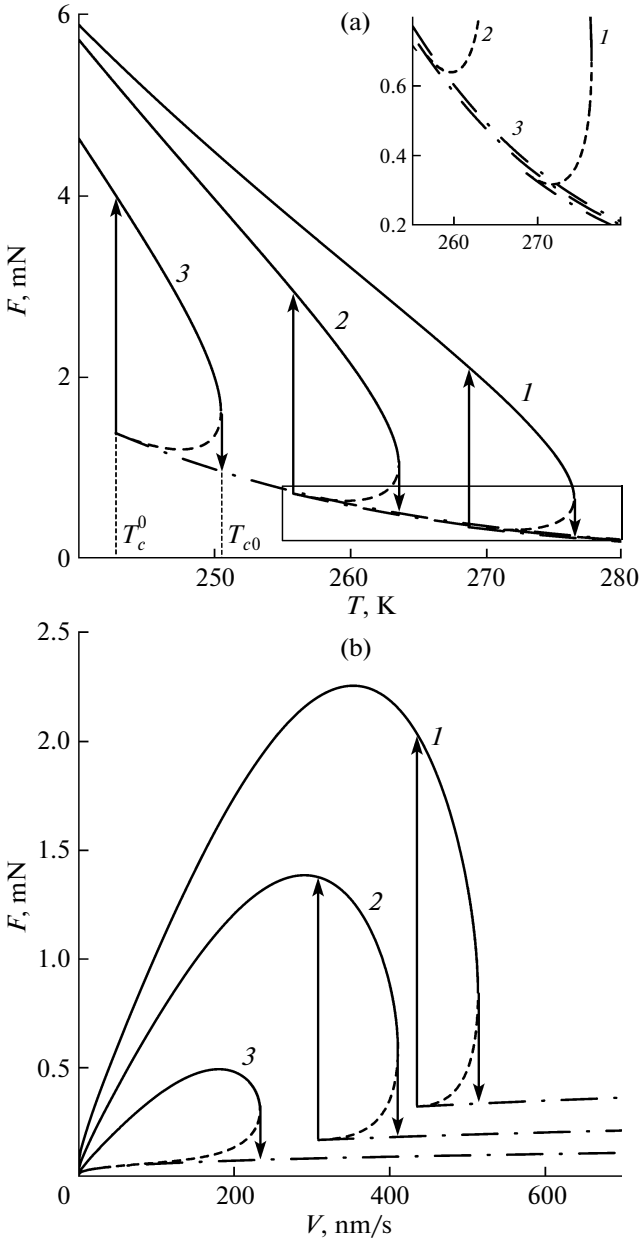

Fig. 3. Dependence of friction force F (17) on temperature T of the friction surfaces and shear velocity V for the same parameters as in Figs. 1 and 2 and $A = 3 \times 10^{-9}$ m^2, $h = 10^{-9}$ m, and $\tau_\varepsilon = 10^{-8}$ s: (a) curves *1–3* correspond to shear velocities $V = 450$, 570, and 670 nm/s, respectively; (b) curves *1–3* correspond to fixed values of temperature $T = 270$, 280, and 292 K, respectively.

decrease in the force of friction upon heating as compared to the results obtained in [21] because not only the elastic, but also the viscous component of the friction force decrease in our case with increasing temperature. In the model [15, 26], in which the temperature dependence of viscosity is also disregarded, the friction force after melting continues to decrease with increasing temperature like in this work, but due to a decrease in the shear modulus that assumes a non-zero value in both phases of the lubricating material. The dependences in Fig. 3a exhibit hysteresis loops because shear modulus (9) changes jumpwise during the first-order phase transition. The inset to the figure shows its enlarged part outlined by the rectangle in the main figure but without the arrows indicating transitions. It can be seen that the $F(T)$ dependences do not coincide after melting for any value of the velocity (the force of friction increases with the velocity). This may occur only due to an increase in viscous stresses (11) upon an increase in the second factor $\dot{\varepsilon} = V/h$ because the elastic component of F becomes zero after melting, and viscosity η_{eff} decreases upon an increase in $V = h\dot{\varepsilon}$.

In accordance with Fig. 3b, the total friction force (17) first increases with velocity due to an increase in viscous σ_v and elastic σ_{el} stresses. Elastic stresses for small values of V increase due to an increase in elastic strain component (15). However, with increasing velocity, shear modulus μ decreases significantly, which ultimately leads to a decrease in the elastic component of F. A critical velocity exists, above which the lubricant is solid-like, but the total friction force begins to decrease.[2] Upon a further increase in the velocity at $V > V_{c0}$ (downward arrow in the figure), the lubricant melts, and elastic stresses (8) become zero, which leads to a jumpwise decrease in F. If we continue to increase the value of V after melting, force F will increase due to the viscous component. The lubricant solidifies with a jumpwise increase in F for a velocity $V < V_c^0$ (upward arrow in the figure). An analogous $F(V)$ dependence is given in [21], but all curves coincide after melting because the temperature dependence of the viscous component of F is not taken into account. Here, we consider a more realistic situation, when an increase in temperature always reduces the friction force. Curve *3* in Fig. 3b differs from all other curves: its solid (stable value of F before melting) and dashed (unstable value of F) segments together form a closed curve. In such a situation, the $F(V)$ dependence after melting (downward arrow) is always described by the dependence represented by the dot-and-dash line because the lubricant cannot solidify upon a decrease in V due to the presence of a potential barrier (curve *2* in Fig. 1) even for zero shear velocity [21].

3. KINETICS OF MELTING

Let us consider the behavior of the mechanical analog of the simple tribological system shown in Fig. 4 using the proposed model [21, 26]. Here, K is the stiffness of the spring and M is the mass of the upper block sliding over a smooth surface separated from it by a

[2] The existence of the maximum on the $F(V)$ dependence for low sliding velocities V in the boundary friction mode was observed experimentally by Tolstoi and Kaplan [1, 27].

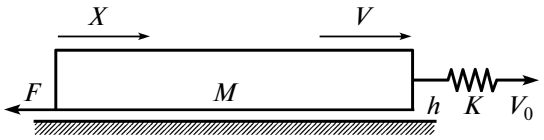

Fig. 4. Diagram of a tribological system.

lubricant layer of thickness h. The free end of the spring is set in motion with velocity V_0. When the block slides over the surface, friction force F (17) appears and decelerates its motion.

The equation for determining coordinate X of the block has the form [3, 12, 21]

$$M\ddot{X} = K\Delta X - F. \quad (18)$$

In this equation, extension ΔX of the spring is defined as

$$\Delta X = \int_0^t V_0 dt' - X, \quad (19)$$

where $t = t'$ is the time of motion of the free end of the spring. Let us write the kinetic relaxation equation of the Landau–Khalatnikov type [21, 28],

$$\dot{\varphi} = -\delta\frac{\partial f}{\partial \varphi}, \quad (20)$$

where we have introduced kinetic coefficient δ. In explicit form, we can write

$$\dot{\varphi} = -\delta(2\alpha(T - T_c)\varphi + a\varphi\varepsilon_{el}^2 - b\varphi^2 + c\varphi^3) + \xi(t). \quad (21)$$

In this expression, we have additionally introduced stochastic term $\xi(t)$ describing small additive fluctuations that should be taken into account in view of peculiarities of the further numerical calculation [20, 21]. In the simplest case, process $\xi(t)$ can be written as white noise with moments

$$\langle\xi(t)\rangle = 0; \quad \langle\xi(t)\xi(t')\rangle = 2D\delta(t - t'), \quad (22)$$

where intensity D of the stochastic source is assumed to be 10^{-25} s^{-1} in further calculations.

Before analyzing the kinetics of the system, we consider the $n(T)$ dependence (Eq. (13)) in graphic form (Fig. 5). Parameter n considerably affects the friction regime that stabilizes in the system shown in Fig. 4. We earlier used the experimentally determined value of $n = 2/3$ [4] in simulation [20, 21]. It follows from Fig. 5 that this value is observed for different alkanes at different temperatures T. Note that viscosity η_{eff}, as well as the melting temperature, increases with the length of the C_nH_{2n+2} molecule. For example, eicosane $C_{20}H_{42}$, for which this dependence is given in Fig. 2, melts at 36.4°C under normal conditions, while the melting point of hectane $C_{100}H_{202}$ is 115.2°C. For ultrathin layers of substances bounded by solid surfaces, these temperatures may differ significantly because they depend on the pressure applied to the surfaces, their structure, and so on. This means that

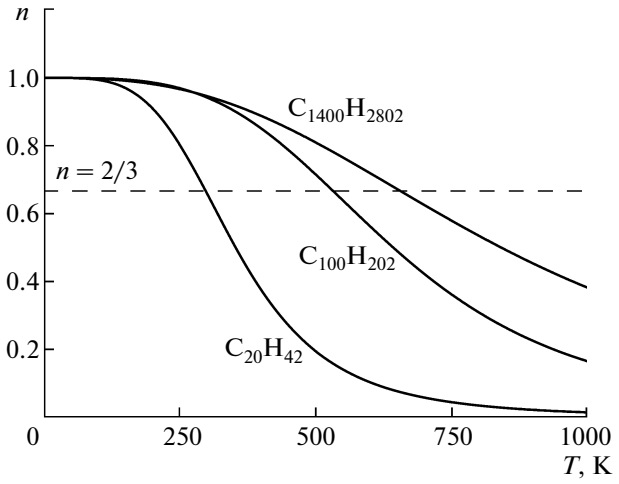

Fig. 5. Dependence of parameter n (dimensionless quantity) on temperature T for three types of lubricant. The values of T_k and β are borrowed from [22]: $C_{20}H_{42}$ (353 K, 4.09), $C_{100}H_{202}$ (642 K, 3.68), and $C_{1400}H_{2802}$ (840 K, 2.79).

analyzing a specific polymer, one has to change the expansion coefficients in potential (1), which can be selected correctly only after additional experiments.

To analyze the kinetics of melting process, we will solve numerically the system of differential equations (18) and (21) taking into account the definitions introduced in Sections 2 and 3. The dependences obtained as a result of solution of these equations are shown in Fig. 6. At a chosen temperature T in the state of rest ($\varepsilon_{el} = 0$), the lubricant is solid-like. At instant $t = 0$, the free end of the spring begins to move uniformly with velocity $V_0 = 2$ μm/s. Friction force (17) increases in this case because velocity V of the upper block increases. The increase in the velocity leads to an increase in elastic strains (15), which results in an increase in the elastic component σ_{el} of stresses (8). Since velocity V is initially much smaller than V_0, the spring is stretched, and extension ΔX increases. When the condition $V > V_{c0}$ is satisfied, the lubricant melts, and stresses σ_{el} assume zero value (lower panel of Fig. 6). Since the elastic component of the friction force becomes zero in this case, the sliding velocity V of the upper block increases significantly. The block rapidly moves over a large distance, which follows from the increase in the slope of the $X(t)$ curve after melting. Since the block now moves with velocity V, which considerably exceeds velocity V_0 of the free end of the spring, the spring is compressed and the value of ΔX decreases. After this, the regime of damped oscillations sets in up to the stabilization of the steady-state sliding of the block with velocity $V = 2$ μm/s coinciding with the velocity V_0 of the free end of the spring. This velocity is much higher than critical velocity V_c^0; for this reason, the lubricant remains liquid-like, thus

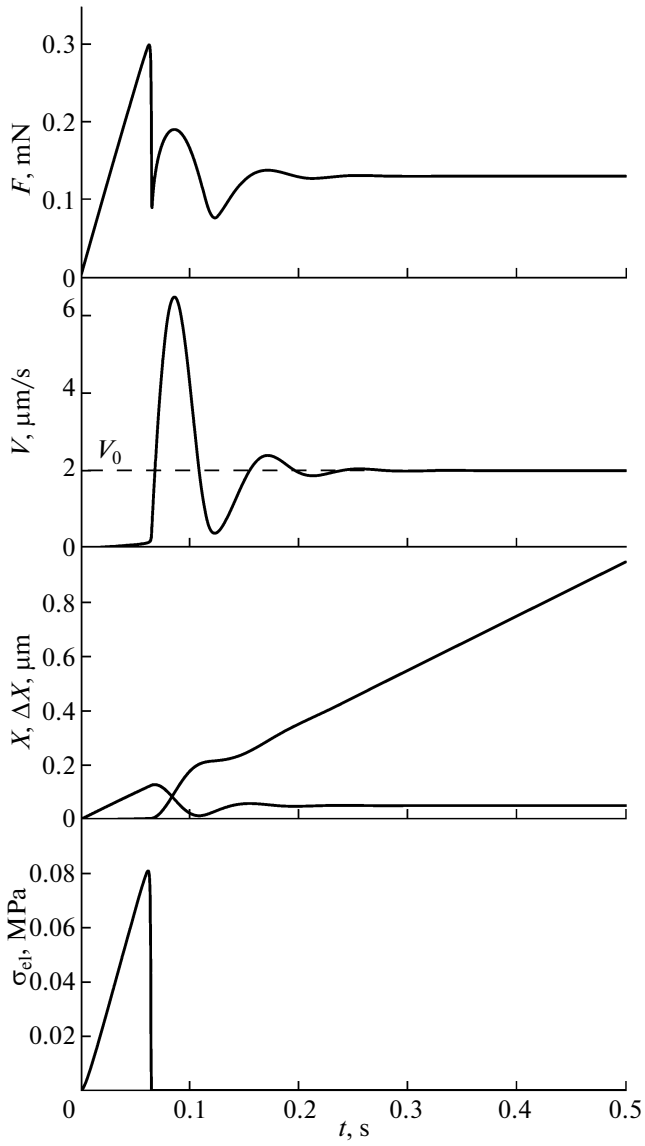

Fig. 6. Dependence of friction force F, shear velocity V of the upper interacting surface, its coordinate X, spring extension length ΔX, and elastic shear stresses σ_{el} on time t for the parameters the same as in Fig. 3 and $M = 0.4$ kg, $K = 2500$ N/m, $\delta = 100$ J^{-1} m^3/s, $T = 295$ K, and $V_0 = 2$ μm/s.

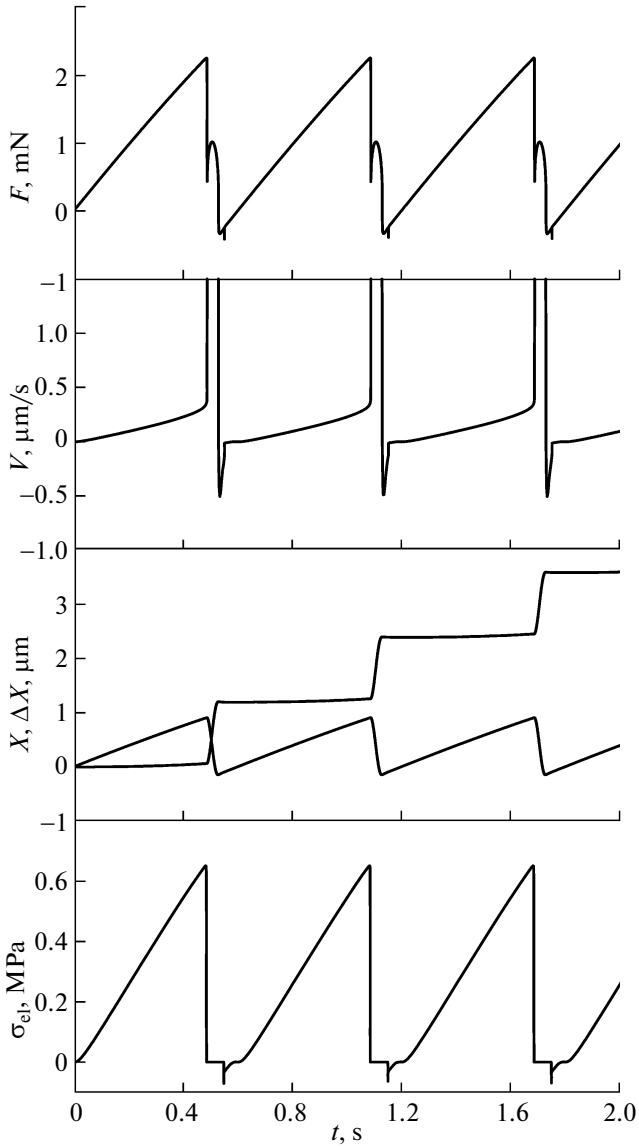

Fig. 7. Kinetic dependences of the quantities under investigation for the same parameters as in Fig. 6 and $T = 270$ K.

ensuring the small value of viscous friction force F. Since a nonzero value of the friction force is sustained during the steady-state motion, the extension of the spring does not relax to zero. It can be determined from Eq. (18), which in the stationary case, leads to the condition

$$K\Delta X = F. \quad (23)$$

In the regime of the steady-state sliding, the time dependence of the coordinate becomes linear because the block moves at constant velocity $V = V_0$. Note that long-term damped oscillations prior to the stabilization of a steady-state sliding were discussed earlier using the synenergetic representation of the lubricant melting [29, 30].

Figure 6 demonstrates the regime in which a steady-state motion of the friction block with a constant velocity stabilizes with time. However, a large number of experimental data indicate that in the boundary friction mode, the interrupted (stick–slip) motion is observed in a wide range of parameters, when the relative velocity of the friction surfaces and the friction force vary with time periodically [3, 31–33]. Such a regime is shown in Fig. 7, which describes the same dependences as in Fig. 6, but at a lower temperature T of the lubricant. At the initial stage of motion, the behavior of the system qualitatively coincides with that shown in Fig. 6. However, melting in this case occurs at a much larger value of extension ΔX of the spring. As

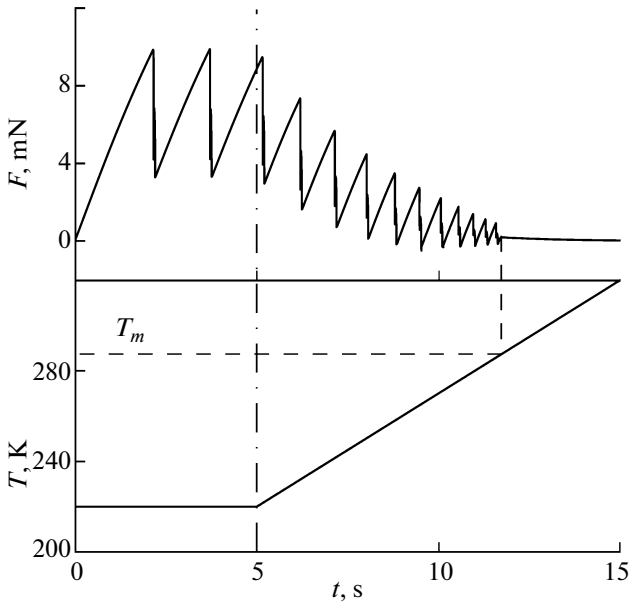

Fig. 8. Dependence of friction force F on time t (upper panel) for the same parameters as in Fig. 6 and upon an increase in temperature T in accordance with the law (24) (lower panel).

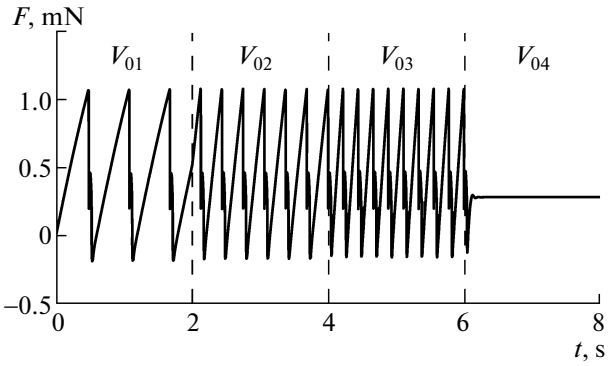

Fig. 9. Dependence of friction force F (17) on time t for the same parameters as in Fig. 8 at temperature $T = 284$ K and velocities $V_{01} = 1$ μm/s, $V_{02} = 2$ μm/s, $V_{03} = 3$ μm/s, and $V_{04} = 4$ μm/s of the free end of the spring.

a result, the moving block after melting acquires a large velocity V that is much higher than velocity V_0 of the free end of the spring. The spring is compressed in this case, and extension ΔX decreases. In the case considered here, the upper block comes to a stop only when the spring is compressed ($\Delta X < 0$) in view of the smallness of the viscous friction force. Then, the spring straightens, which leads to the motion of the upper friction surface in the opposite direction with velocity $V < 0$; the friction force also becomes negative in this case. After the repeated change in the direction of motion ($V > 0$) occurring due to stretching of the spring and an increase in the elastic driving force $K\Delta X$, the lubricant solidifies, and then the process described above is repeated. Thus, a periodic regime of stick–slip friction sets in. On the time dependences of the friction force shown in Figs. 6 and 7, the peak of $F(t)$ is observed after melting and a subsequent sharp decrease of the friction force; the reasons for this peak are considered in detail in [21].

To reveal the features of the effect of lubricant temperature T on the regime of operation of a tribological system, Fig. 8 shows the time dependence of the friction force under a gradual increase in temperature in accordance with the law

$$T\,(\mathrm{K}) = \begin{cases} 220, & t < 5\ \mathrm{s} \\ 170 + 10t, & t \geq 5\ \mathrm{s}. \end{cases} \qquad (24)$$

At the initial stage, the temperature remains unchanged; therefore, a stationary regime of the stick–slip motion with a saw-tooth dependence $F(t)$ is observed. Since the temperature is low as compared to that in Fig. 7, the friction force in the given case is larger and is always positive (i.e., the spring is always stretched during motion, $\Delta X > 0$), and the block moves in the same direction. Further, we linearly increase the temperature ("heat" the lubricant), which leads to a decrease in the effective viscosity (12) (see Fig. 2) and to a corresponding decrease in the friction force; for this reason, when the temperature exceeds a certain value, regions with $F < 0$ appear (see the explanation to Fig. 7). The figure shows the temperature T_m above which the lubricant melts completely and steady-state sliding regime sets in. Temperature T_m differs from (4) because we consider here a more complicated case, and the value of T_m is affected by parameters such as spring stiffness K and mass M of the block. It should be noted that an increase in the temperature of the lubricant in Fig. 8 leads to an increase in the frequency of phase transitions, which was demonstrated earlier in [20, 21, 26]. However, in contrast to these publications, the kinetic value of the friction force (minimal value of F over a period) in our case considerably decreases with increasing temperature in the stick–slip regime. This effect can be explained by the fact that we take into account the decrease in lubricant viscosity η_{eff} with increasing temperature.

Figure 9 shows the time dependence of the friction force with a gradual increase in velocity V_0. It can be seen that with increasing velocity, the frequency of melting/solidification phase transitions increases. This is due to the fact that the critical value of elastic stresses for which the lubricant melts is attained sooner at high velocities. Correspondingly, melting begins earlier, and the system can perform a larger number of phase transitions between the structural states of the lubricant during the same time interval. For velocity $V_0 = V_{04}$, the lubricant melts completely, and the kinetic regime of sliding with a constant friction force sets in. Since the dependences in Fig. 9 are plotted for a fixed temperature T, the curves qualitatively repeat analogous dependences given in [21, 26].

CONCLUSIONS

In this study, a theoretical model is proposed for describing boundary friction in the presence of an ultrathin film of a lubricating material between two atomically smooth surfaces. It is shown that the stick–slip friction mode, which is often observed experimentally in such systems, appears due to the first-order phase transition between the structural state of the lubricant. This study makes it possible to extend the results of previous investigations because it takes into account the temperature dependence of viscosity for polymer pseudoplastic lubricating materials. The effect of the lubricant temperature and shear velocity on the stick–slip regime is analyzed. It is shown that upon an increase in temperature, the reversive motion regime can set in after melting, and long-term oscillations can exist up to stabilization of a steady-state sliding. Our results coincide qualitatively with available experimental data. The model is quantitative and can be employed for describing a wider range of conditions of boundary friction whenever required. For example, this model can be used for describing processes occurring during friction between rough surfaces because the description contains the thickness of the lubricant, which will assume different values on the plane of contact and will vary in the course of motion.

ACKNOWLEDGMENTS

This study was supported in part by the Ministry of Education and Science of Ukraine under the project no. 0112U001380 "Modeling of Friction for Metal Nanoparticles and Boundary Liquid Films Interacting with Atomically Smooth Surfaces." The work was supported by the grant of the Cabinet of Ukraine.

REFERENCES

1. A. S. Akhmatov, *Molecular Physics of Boundary Friction* (Fizmatgiz, Moscow, 1963; Israel Program for Scientific Translations, Jerusalem, 1966).
2. B. N. J. Persson, *Sliding Friction: Physical Principles and Applications* (Springer, New York, 2000).
3. H. Yoshizawa and J. Israelachvili, J. Phys. Chem. **97**, 11300 (1993).
4. G. Luengo, J. Israelachvili, and S. Granick, Wear **200**, 328 (1996).
5. A. D. Berman, W. A. Ducker, and I. N. Israelachvili, Langmuir **12**, 4559 (1996).
6. S. Yamada, Langmuir **21**, 8724 (2005).
7. S. Ohnishi, D. Kaneko, J. Ping Gong, Y. Osada, A. M. Stewart, and V. V. Yaminsky, Langmuir **23**, 7032 (2007).
8. S. Yamada, Langmuir **24**, 1469 (2008).
9. O. M. Braun and A. G. Naumovets, Surf. Sci. Rep. **60**, 79 (2006).
10. I. M. Sivebaek, V. N. Samoilov, and Bo N. J. Persson, Langmuir **26**, 8721 (2010).
11. M. O. Robbins and M. H. Muser, "Computer Simulations of Friction, Lubrication and Wear," *Modern Tribology Handbook*, Ed. by B. Bhushan (CRC, Boca Raton, 2001), pp. 717–765; cond-mat/0001056.
12. V. L. Popov, Tech. Phys. **46**, 605 (2001).
13. V. L. Popov, Solid State Commun. **115**, 369 (2000).
14. A. E. Filippov, J. Klafter, and M. Urbakh, Phys. Rev. Lett. **92**, 135503 (2004).
15. I. A. Lyashenko, A. V. Khomenko, and L. S. Metlov, Tech. Phys. **55**, 1193 (2010).
16. A. V. Khomenko and I. A. Lyashenko, J. Phys. Studies **11**, 268 (2007).
17. A. V. Khomenko, I. A. Lyashenko, and V. N. Borisyuk, Ukr. J. Phys. **54**, 1139 (2009).
18. A. V. Khomenko, I. A. Lyashenko, and V. N. Borisyuk, Fluct. Noise Lett. **9**, 19 (2010).
19. L. D. Landau and E. M. Lifshitz, *Course of Theoretical Physics*, Vol. 5: *Statistical Physics* (Nauka, Moscow, 1995; Pergamon, Oxford, 1980).
20. I. A. Lyashenko, Tech. Phys. **56**, 869 (2011).
21. I. A. Lyashenko, Tech. Phys. **57**, 17 (2012).
22. I. M. Sivebaek, V. N. Samoilov, and B. N. J. Persson, Phys. Rev. Lett. **108**, 036102 (2012).
23. V. L. Popov, Tech. Phys. Lett. **25**, 815 (1999).
24. I. A. Lyashenko, Tech. Phys. **56**, 701 (2011).
25. G. I. Epifanov, "Dependence of friction force on normal load," in *Dry Friction: Collection of Scientific Works* (Akad. Nauk Latv. SSR, Riga, 1961).
26. I. A. Lyashenko, A. V. Khomenko, and L. S. Metlov, Tribol. Int. **44**, 476 (2011).
27. D. M. Tolstoi and R. L. Kaplan, in *Theory of Friction and Wear: Collection of Scientific Works* (Nauka, Moscow, 1965), pp. 44–49.
28. L. D. Landau and E. M. Lifshits, Dokl. Akad. Nauk SSSR, **96**, 469 (1954).
29. A. V. Khomenko and Ya. A. Lyashenko, Tech. Phys. **55**, 26 (2010).
30. A. V. Khomenko and I. A. Lyashenko, J. Friction Wear **31**, 308 (2010).
31. J. Israelachvili, Surf. Sci. Rep. **14**, 109 (1992).
32. A. L. Demirel and S. Granick, J. Chem. Phys. **109**, 6889 (1998).
33. G. Reiter, A. L. Demirel, J. Peanasky, L. L. Cai, and S. Granick, J. Chem. Phys. **101**, 2606 (1994).

Translated by N.V. Wadhwa